ISSN 0006-2979, Biochemistry (Moscow), 2008, Vol. 73, No. 1, pp. 56-64. © Pleiades Publishing, Ltd., 2008.
Published in Russian in Biokhimiya, 2008, Vol. 73, No. 1, pp. 69-79.
Originally published in Biochemistry (Moscow) On-Line Papers in Press, as Manuscript BM07-204, October 14, 2007.

Molecular Modeling Studies of Substrate Binding by Penicillin Acylase

G. G. Chilov[1], O. V. Stroganov[2], and V. K. Švedas[1,2]*

[1]Belozersky Institute of Physico-Chemical Biology and [2]Faculty of Bioengineering and Bioinformatics, Lomonosov Moscow State University, 119991 Moscow, Russia; fax: (495) 939-2355; E-mail: vytas@belozersky.msu.ru

Received June 25, 2007
Revision received August 3, 2007

Abstract—Molecular modeling has revealed intimate details of the mechanism of binding of natural substrate, penicillin G (PG), in the penicillin acylase active center and solved questions raised by analysis of available X-ray structures, mimicking Michaelis complex, which substantially differ in the binding pattern of the PG leaving group. Three MD trajectories were launched, starting from PDB complexes of the inactive mutant enzyme with PG (1FXV) and native penicillin acylase with sluggishly hydrolyzed substrate analog penicillin G sulfoxide (1GM9), or from the complex obtained by PG docking. All trajectories converged to a similar PG binding mode, which represented the near-to-attack conformation, consistent with chemical criteria of how reactive Michaelis complex should look. Simulated dynamic structure of the enzyme–substrate complex differed significantly from 1FXV, resembling rather 1GM9; however, additional contacts with residues bG385, bS386, and bN388 have been found, which were missing in X-ray structures. Combination of molecular docking and molecular dynamics also clarified the nature of extremely effective phenol binding in the hydrophobic pocket of penicillin acylase, which lacked proper explanation from crystallographic experiments. Alternative binding modes of phenol were probed, and corresponding trajectories converged to a single binding pattern characterized by a hydrogen bond between the phenol hydroxyl and the main chain oxygen of bS67, which was not evident from the crystal structure. Observation of the trajectory, in which phenol moved from its steady bound to pre-dissociation state, mapped the consequence of molecular events governing the conformational transitions in a coil region a143-a146 coupled to substrate binding and release of the reaction products. The current investigation provided information on dynamics of the conformational transitions accompanying substrate binding and significance of poorly structured and flexible regions in maintaining catalytic framework.

DOI: 10.1134/S0006297908010082

Key words: penicillin acylase, substrate binding, molecular modeling, conformational flexibility

Penicillin acylases (PA) (EC 3.5.1.11) are of interest first of all due to their ability to hydrolyze natural penicillin G (PG) selectively yielding 6-aminopenicillanic acid [1]. Further investigations revealed that PA specificity towards both aminic and acidic counterparts of the substrates is substantially broader [2, 3]. Nowadays penicillin acylases are industrially important enzymes for large-scale production of antibiotic nuclei [4], but there are good grounds to believe that the biocatalytic potential of these enzymes for synthesis of new penicillins and cephalosporins is just in its infancy. Moreover, perspectives of PA catalysis are not restricted just to antibiotic chemistry due to extremely high stereospecificity in the hydrolysis of N-acylated derivatives of natural and non-conventional amino acids [5], high acyltransferase activity in alkaline aqueous medium [6], and ability to perform effective hydrolysis or acylations in acidic aqueous medium [7-9]. Unique catalytic properties of PAs make fundamental study of their catalytic machinery highly attractive.

In spite of the fact that studies of PA started in the early 60s, and a huge array of experimental data has accumulated since, it has been only recently that structural studies have attracted wide fundamental interest to PA catalytic mechanism. Analysis of the crystal structure [10, 11] provided evidence that the active site of the enzyme lacks such residues as histidine and aspartate/glutamate, which comprise the classical catalytic triad of serine hydrolases. Catalytically active serine was found at the N-terminus of the heterodimeric PA b-chain, and it was

Abbreviations: MD) molecular dynamics; PA) penicillin acylase; PG) penicillin G; PGSO) penicillin G sulfoxide; RHF) Restricted Hartree–Fock method; RMSD) root mean square deviation; RMSF) root mean square fluctuation.

* To whom correspondence should be addressed.

inferred that it is the free amino group of the serine that can activate its own hydroxyl. This observation suggested a name, N-terminal nucleophile (Ntn) hydrolases, to the newly discovered group of enzymes with PA being the most studied family member so far.

Analysis of a set of crystal structures of PA complexes with its inhibitors allowed mapping of the enzyme active site [12]. A compact acyl group binding pocket was located at the very bottom of a broad funnel-like depression on the protein interface. It was found that a pair of residues, aF146 and aR145, forming one of the sides of the hydrophobic pocket and its bottleneck, can adopt two principally different conformations [12]. The so-called "closed" conformation was observed in PA complexes with specific inhibitors: in this state, side chains of aF146 and aR145 are in close contact with the ligand. In the alternative, "open" conformation, which is characterized by side chain radicals of aF146 and aR145 shifted towards the solution, the enzyme–ligand contacts are loosened. The enzyme adopts "open" conformation upon binding of nonspecific, bulky inhibitors. It was evident that the structurally flexible region of the PA active site plays an important role in the mechanism of recognition and binding of the substrates and inhibitors. According to a set of resolved structures [12], the size of the bottleneck, separating the hydrophobic pocket from the solution, is not large enough to encompass the phenyl ring—the structural fragment of the most specific inhibitors of PA. Thus, it may be inferred that flexibility of residues aF146 and aR145 is exploited accommodating an arbitrary, even specific, substrate in the active site. However, the role of the active site conformational mobility in substrate binding is still a guess-work, which needs novel clues extending static information provided by crystallographic studies.

For mechanistic studies, it is very important to locate residues involved and responsible for enzyme–substrate interactions in a Michaelis complex, especially those standing for specificity towards the leaving group of the substrate. In this respect, two attempts [13, 14] have been taken to deduce the structure of the enzyme complex with one of its best substrates, PG (Fig. 1a, see color insert).

Since fully fledged X-ray analysis of the intact enzyme–substrate complex was not possible due to rapid hydrolysis of the substrate, some tricks were made to imitate the Michaelis complex. The structure 1FXV [13] comprises the complex of the inactive mutant enzyme with the PG, while the structure 1GM9 [14] comprises a complex of the native PA with the sluggishly hydrolyzed substrate analog penicillin G sulfoxide (PGSO) (Fig. 1b). X-Ray structures showed similar organization of the acyl moiety binding pocket but substantially different binding patterns of the leaving group of the substrate.

Actually, this situation reflects a genetic trait of a crystallographic experiment: the static picture of the complex of the native enzyme with a non-reactive substrate analog (or inactive enzyme with a "real" substrate) is merely a starting point in the study of the molecular principles of enzymatic catalysis—an intrinsically dynamic phenomenon. Searching for an approach to overcome these limitations, we set our hopes on molecular modeling, which, being adequately applied, could extend our understanding of the enzyme–substrate interactions based on available experimental and structural data. From this point of view, PA seems to be a very promising object for molecular modeling, since a lot of available experimental information still lacks proper comprehension at the molecular level. In this work combined molecular docking and molecular dynamics approach was applied to remedy shortcomings and ambiguities of available crystallographic data and to extend our understanding of at least some aspects of PA substrate specificity.

METHODS OF INVESTIGATION

Constructing systems for molecular dynamics (MD) simulations. Molecular dynamics studies of PA from *E. coli* and its complexes with substrates and inhibitors were based on either available X-ray [12-14] or docked structures. Before MD simulation was run, several preparatory procedures were performed. A few residues at the termini of the a-chain of the enzyme, which were not resolved in X-ray studies, were built using Swiss-PdbViewer v.3.7. Mutation bN241A present in 1FXV [13] was manually repaired. The protonation state of Asp, Glu, Lys, and Arg was chosen ionized; placing of functional hydrogen atoms on histidine residues followed a special algorithm accounting for possible hydrogen bonds and estimated pK_a values. Total charge of the protein was zero, reflecting its state at neutral pH (experimentally determined isoelectric point being 6.9 for PA from *E. coli*). MD simulations were performed in explicit aqueous medium with the protein immersed in the box of water molecules. The box dimensions were set in such a way that the minimal distance between protein and the box wall was 1.5 nm. Superfluous water molecules that were trapped inside the protein due to inaccuracy of the box filling algorithm were manually removed, so that only crystallographic water molecules remained in the protein interior.

MD protocol. All MD calculations were done with the Gromacs package (www.gromacs.org) [15, 16] in all atom OPLS [17] force field and TIP3P [18] water. The equations of motions were integrated with 4 fsec time step. The highest frequency motions were eliminated by dummy atoms constructions [19]. Simulations were performed at a constant volume and at 300 K using the Berendsen thermostat with 0.1 psec relaxation time. All bonds were constrained during the simulation using the LINCS algorithm [20]. Periodic boundary conditions were used to account for the continuum solution. Forces

were calculated with the twin range cut-off with 9 Å to account for the short range and 15 Å for the long range interactions. The long range list was updated each 20 fsec. Electrostatics were treated via reaction field methodology [21] with dielectric permeability of 80 and 15 Å cut-off; and van der Waals interactions were smoothly set to zero at 9 Å distance. Before the unconstrained MD in solution was run, the system was subjected to several pre-equilibration steps. First, the entire system was energy-minimized using steepest descent interspersed with conjugated gradient algorithm to a force threshold of 1 kcal·mol^{-1}/Å. After that the system was heated to 300 K in 100 psec, preserving restraints on the protein coordinates. During the following 400 psec, restraints on the protein coordinates were stepwise released, and the unconstrained dynamics in explicit solution was launched.

MD parameterization of PG. Molecular mechanical parameters of the PG were adapted from *ab initio* quantum chemical calculations performed on an analogous compound—N-acetyl-6-aminopenicillanic acid. Equilibrium geometry search, single point energy calculations, and electrostatic potential evaluation were performed at the Restricted Hartree–Fock (RHF) level in 6-31G* basis using PC GAMESS software [22, 23]. Partial atomic charges were assigned on the basis of *ab initio* calculations within the scopes of RESP methodology [24] and previously derived set of charges for 6-aminopenicillanic acid [25]. Dependence of energy on the torsion angle of rotation around the C–N bond connecting the β-lactam ring and the amide group of penicillin was calculated by quantum chemistry methods and the resulting energy profile was used in subsequent MD simulations.

Molecular docking. AutoDock 3.05 software (http://www.scripps.edu/pub/olson-web/doc/autodock/) was used for construction of several molecular systems by molecular docking. Docking was performed with the options of combined genetic algorithm and local search [26]. Normally, 20 independent runs were parsed with 50 starting conformations in each run and maximum number of generation equal to 27,000. Resulting conformations were clustered with the threshold of 0.5 Å.

RESULTS AND DISCUSSION

General traits of MD trajectories. During unconstrained molecular dynamics in explicit aqueous solution, all systems revealed steady behavior. Root mean square deviation (RMSD) of the protein from its starting (X-ray) structure reached an equilibrium level of 1.6 Å in 1.5 nsec, and root mean square fluctuation (RMSF) was about 0.5 Å. It turned out that mainly the residues on the protein interface have the stipulated observed mean deviation and fluctuation magnitudes, while RMSD and RMSF of the active site residues were significantly lower (Fig. 2).

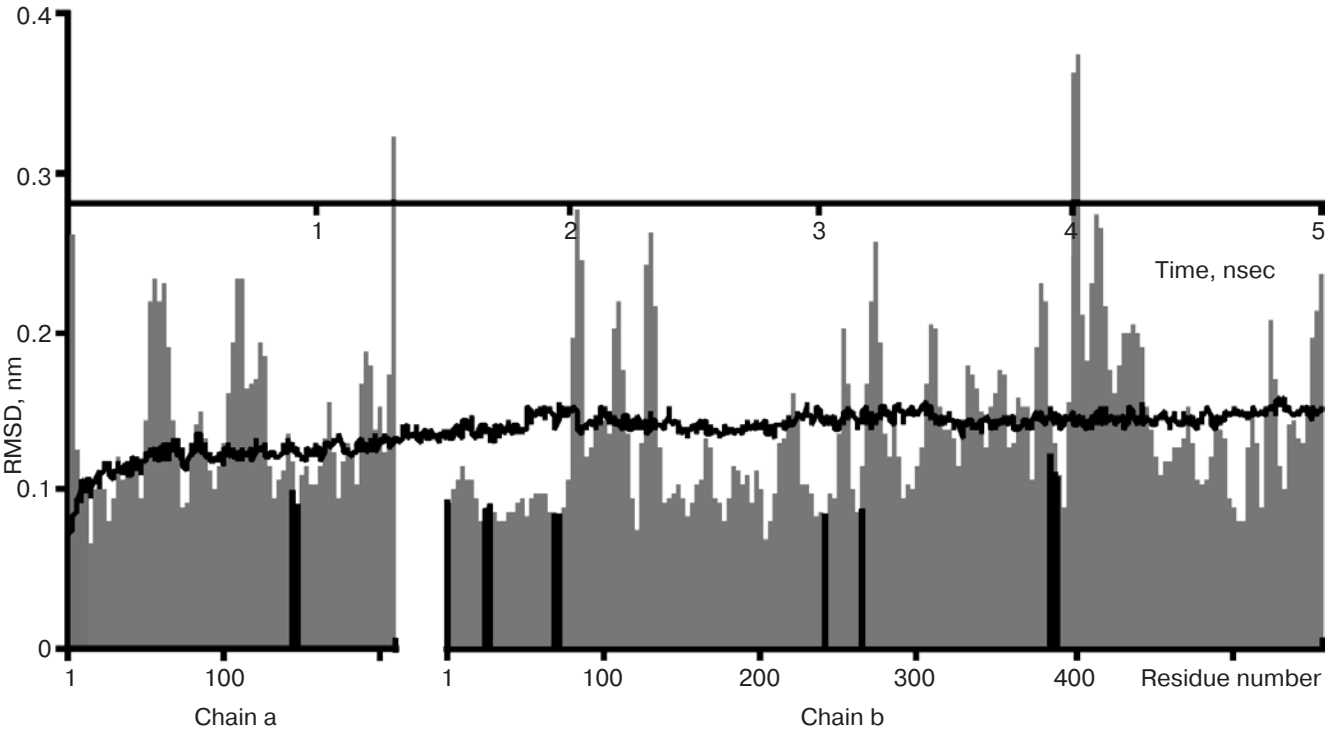

Fig. 2. Root mean square deviations from the starting structure for free enzyme simulation (black curve) and dependence of the RMSD on residue number (gray area). Active site residues are shown in black vertical lines.

Thus, upon transition from the crystal lattice to aqueous medium no global conformational change was observed, suggesting X-ray structure to be a good starting point for modeling the behavior of the protein in a solution.

Subtle organization of the active site and specific interactions. During the MD run several presumably crucial for catalysis hydrogen bonds between hydrogens of bS1 amino group and side chain oxygens of bQ23 and bN241 were observed. These hydrogen bonds were firm and their occupancies were 78 and 98% of the trajectory time. These interactions, while not seen by X-ray, but revealed by MD simulations, orient the amino group of the catalytic bS1 in such a way that its lone electron pair faces the side chain hydroxyl hydrogen of serine thus making proton transfer and nucleophilic attack possible. Another observation concerns hydrogen bonding of bS1 hydroxyl group. According to 1GK9, there should be a hydrogen bond between the main chain amide of bQ23 and bS1 hydroxyl oxygen. This hydrogen bond was also found in the MD trajectory of the free protein, but after 800 psec of the simulation bS1 hydroxyl oxygen has formed two new bonds with the backbone amide of bA69 and the side chain amide of bN241. This came with the conformational transition of the bS1 side chain from gauche-(+) to gauche-(–).

Enzyme–PG complex. Direct crystallographic studies of PA with its substrates, especially with PG, are not possible due to rapid hydrolysis of the substrate. That is why several strategies have been elaborated to mimic enzyme–PG complex. One of them, proposed by the research group from Groningen [13], used inactivated enzyme bearing single point mutation in the active site (Protein Data Bank ID 1FXV). Alternatively, structural biologists from York [14] exploited native enzyme and PG analog, PGSO (Fig. 1b), which, in fact, was a very poor penicillin acylase substrate (Protein Data Bank ID 1GM9).

We have performed analysis of both structures, considering the requirements of the theoretical chemistry to the structure of reactive enzyme–substrate complex. Intent examination of 1FXV revealed its inconsistency as a model of a Michaelis complex: serine hydroxyl oxygen and carbonyl carbon of the substrate are positioned in such a way that chemical reaction can not proceed *per se* without further rearrangements. Due to the introduced mutation of bN241A interactions of the substrate with oxyanion hole residues—main chain amide of bA69 and side chain amide of bN241—are distorted leading to loosened substrate contacts with the enzyme. Another structure, 1GM9, was more chemically consistent: serine hydroxyl and PGSO amide bond are already in a near attack conformation, and carbonyl oxygen of the ligand is trapped in the oxyanion hole. The authors suggested [14] that it was one surplus internal hydrogen bond between the amide and the sulfonyl oxygen that stabilizes a planar amide bond, preventing the further formation of the tetrahedral intermediate upon serine nucleophilic attack, while other protein–ligand interactions with this pseudo substrate remained the same as in a "true" Michaelis complex. However, along with the mentioned hydrogen bond there is a noticeable difference between the thiazolidine ring conformations of PG and its oxidized analog (Fig. 1c), which might, in fact, influence the binding mode of the ligand. Finally, it is confusing that the binding pattern of the PG leaving group, the most undisclosed aspect of the enzyme–substrate interactions so far, appears to be significantly different in two reported X-ray structures (1FXV and 1GM9).

To clarify the mechanism of the PG binding in the active site of the enzyme, we have applied molecular modeling techniques to study three molecular systems modeling Michaelis complex. The first (ES1) was based on 1FXV structure, the second (ES2) on 1GM9 structure, and the third (ES3) was obtained by docking the PG molecule to the protein borrowed from 1PNL [10]. To construct fully functional Michaelis complex, bA241 in ES1 was resubstituted to Asn. In ES2, substrate analog was changed to PG with the initial position of penicillin G taken from sulfoxide coordinates. Conformation of the substrate in ES3 was chosen as the most energetically favorable pose found in multiple docking experiments. As it can be seen from Fig. 3 (see color insert), starting conformations and binding modes of PG differ within ES1, ES2, and ES3, but the latter two look very much alike.

Analysis of RMSDs of the active site residues in the Michaelis complex revealed that upon PG binding no conformational transition takes place. The largest displacement of the substrate from its initial position takes place in ES1 trajectory (Fig. 3), when the thiazolidine ring of the substrate shifts to a new position in the active site. Conformation of the PG in the ES2 model undergoes the smallest, but still noticeable changes. However, the most important observation is that all three trajectories converge to practically the same binding pattern of the leaving group of the substrate (Fig. 3b and Table 1).

In 1FXV structure (prototype for the ES1 simulation system) penam ring of the substrate had contacts with aF146 and bF71 and leaned on two residues, aR145 and aF146, which underwent a conformational transition upon substrate binding and switched to an "open" conformation. However in ES1, when the mutation making enzyme inactive has been repaired and the system was subjected to molecular dynamics, the leaving group of PG moved to the opposite side of the active site funnel and formed contacts with bR263 and bN388. On the contrary, penicillin β-lactam moiety in 1GM9 and docked structures has been initially placed in the vicinity of bR263 and bN388 residues. During MD simulation, leaving group of the substrate has loosened its interactions with the protein and shifted towards solution, retaining, however, contacts with these residues. This difference between the X-ray

Table 1. Hydrogen bonds and van der Waals contacts between substrate and enzyme in starting (X-ray) structures and MD trajectories

Contacts	Starting (X-ray) structure*			MD structure**		
	ES1	ES2	ES3	ES1	ES2	ES3
	Hydrogen bonds					
Substrate CO group						
bA69 main chain amide	–	+	+	–	1.0	0.9
bN241 side chain amide	–	–	+	0.03	0.9	0.9
β-lactam COO^- group						
bN388 side chain amide	–	–	–	–	0.3	–
	Van der Waals contacts					
aR145	+	–	–	0.5	0.9	1.0
bR263	–	–	+	0.5	0.9	1.0
bT384	–	–	–	0.5	–	0.03
bQ385	–	–	–	0.9	0.6	0.4
bS386	+	+	+	0.7	0.9	0.6
bN388	–	+	+	0.3	1.0	0.6

* Plus or minus denotes the presence or absence of the corresponding contact.
** Number denotes relative occupancy of the contact along the trajectory.

structure and the dynamic picture might arise because of imperfectness of the PGSO as a model of native substrate, penicillin G. Another clue comes from the entropic considerations, according to which binding of the leaving group is steered by the balance between static and stiff, on one hand, and more loose and flexible, on the other hand, contacts with the protein. This balance favors substrate mobility at higher temperature, which is the case while comparing 1GM9 structure, resolved at 120 K, and those of ES2 and ES3 simulated at room temperature.

Chemically it is anticipated that Michaelis complex should represent so-called "near attack" conformation, in which a substrate is capable of undergoing reaction without further rearrangements. To meet this requirement, conformation of the enzyme–substrate complex should fit several geometric restraints dictated by the catalytic mechanism of penicillin acylase. This mechanism, first proposed in [10] and recently verified by quantum chemical calculations [27], assumes that the amino group of the N-terminal serine participates in proton abstraction from its own hydroxyl group increasing its nucleophile reactivity. To make proton transfer viable, serine amino group should be oriented with its lone electron pair towards the hydroxyl hydrogen, and atoms Oγ and N of bS1 should stay quite close to each other. Another restraint is imposed on the relative positions of the carbonyl carbon of the substrate and the serine hydroxyl oxygen: for the nucleophilic attack to happen, atoms should stay in a van der Waals contact, and the angle between the amide group plane of the substrate and the O(serine)–C(substrate) vector should be in the vicinity of 90°. Another condition concerns hydrogen bonding of the substrate carbonyl oxygen by the main chain amide of bA69 and the side chain amide of bN241—residues forming the so-called oxyanion hole. It appears that the enzyme–substrate complexes simulated in ES2 and ES3 trajectories satisfy all the criteria of the near-attack conformation. Both hydrogen bonds with the oxyanion hole are present with the average occupancies close to unity (Table 1), distance distribution between the reacting atoms shows that carbonyl carbon of the substrate and serine hydroxyl oxygen stay in close van der Waals contact, and their relative orientation is proper for the nucleophilic attack during the whole trajectory (Fig. 3, c and d). Orientation of the amino group is kept proper for the proton transfer by means of two hydrogen bonds with the side chain oxygen atoms of bN241 and bQ23.

Quite different is the situation with ES1 trajectory evolved from 1FXV structure. The distance between the hydroxyl oxygen and the carbonyl carbon of the substrate is about 1 Å longer than in ES2 and ES3, and orientation of the substrate amide plane is inconsistent with the nucleophilic attack (Fig. 3, c and d). This is due to formation of the "non-productive" hydrogen bond between the serine hydroxyl and substrate carbonyl group, which shields reacting atoms from each other. At the same time,

no hydrogen bonds with the oxyanion hole are formed (Table 1). Thus, during 10 nsec MD simulation of ES1 structure substrate is not trapped to near attack conformation, and 1FXV with its "mortal" mutation can hardly be considered as an adequate model for the Michaelis complex. In addition to structural information, molecular dynamics simulations can provide energy terms associated with protein–ligand interactions (Table 2).

It clearly follows that the strongest interaction in the enzyme–substrate complex is due to bR263, whose positively charged guanidine group is in a close contact with PG carboxylic group. Also considerable, however, to a lesser degree, is interaction with another positively charged residue, aR145. These figures reflect the fact that during molecular dynamics trajectory carboxylic group of PG remained closer to bR263 than to aR145 with average minimal distances between groups equal to 4.3 and 6.2 Å, correspondingly. Discussion on the role of the positive charge in substrate binding by PA has a long history. When crystal structure of the enzyme and its complexes with competitive inhibitors, derivatives of phenylacetic acid [10], became available, it appeared that there were at least two positively charged residues, bR263 and aR145, in a direct proximity to the active site. The situation turned even more complicated when two crystal structures modeling enzyme–substrate complex had been reported—one of them ascribed a crucial role in PG binding to aR145 [13], while another pointed to bR263 [14]. The current investigation does not claim that the role of the positive charge in PA active center is completely settled; however, it rigorously states that in case of PG binding one of the arginine residues, namely bR263, contributes more.

It should be specially noted that molecular dynamics studies exposed several new residues whose role in PG binding was not discussed previously. These residues, bG385 and bN388, are located at the active site funnel interface (Fig. 4, see color insert). In both 1FXV and 1GM9 structures residue bN388 is placed with its side chain carbonyl oxygen towards solution, but during the molecular dynamics run it flips to expose its amide group and form a contact with carboxylic group of the substrate. Formation of this contact, not present in X-ray structure, was also facilitated by change of the penam ring conformation while switching from the oxidized to the native penicillin form. Interaction with bG385 is not direct, and rather mediated by a bridging water molecule, but energetic estimations still show its significance. Thus, molecular dynamics studies have outlined weak spots of crystallographic experiments and allowed refining and extending our knowledge about substrate binding in the active site of PA.

Enzyme–phenol complex. Another intriguing question that was raised by experimental studies and seemed to need further inferences on a qualitatively new level concerned phenol binding in the active site of PA. Experimental studies [28] of alcohol binding by PAs from two sources, *E. coli* and *Alcaligenes faecalis*, revealed rather good correlation between the alcohol hydrophobicity and its binding energy. It was only phenol whose binding energy was 2 kcal/mol more advantageous than followed solely from its hydrophobicity. The same observation held true for both enzymes, and thus led to suggestion that it is an extra, conservative, and specific interaction, which places phenol in such an exceptional state. It was suggested [28] that it might be an additional hydrogen bond, but from the X-ray experiment [12] it followed that the phenol molecule was oriented with its hydroxyl group towards the bottom of the hydrophobic pocket, and no hydrogen bonds could be detected. To be more precise, the phenol hydroxyl was placed in vicinity of the side chain oxygen of bS67, but the distance between these groups (3.5 Å) was too large for hydrogen bonding. However, even this distance was estimated wrong for whatever reason and hydrogen bond with Oγ of bS67 could take place that would not explain specific interactions with PA from *A. faecalis*, which has an alanine instead of a serine at this position.

Table 2. Energies (in kJ/mol) of PG interaction with enzyme active site residues averaged over entire MD trajectories

Residue	ES1	ES2	ES3
aR145	–12.8	–38.7	–47.0
aF146	–23.5	–22.0	–19.5
bS1	–21.4	–21.9	–18.3
bF24	–18.2	–10.0	–17.3
bA69	–16.4	–26.2	–24.5
bF71	–9.8	–8.9	–9.0
bR263	–55.1	–83.6	–75.2
bN241	–5.3	–24.2	–26.0
bG385	–31.9	–22.0	–15.9
bN388	–18.8	–17.8	–26.4

To investigate interactions of PA with phenol, molecular complexes EL1-EL4 were constructed. EL1 structure was transferred directly from PDB (1AI7) and treated according to the molecular dynamics setup described above. EL2 and EL3 were fished out from the results of multiple phenol docking to the energy-minimized 1AI7; EL4 was also a docked structure, but the protein was taken after pre-equilibration of EL1 system at 300 K. Constructed systems differed in their hydrogen bonding patterns: EL1 lacked hydrogen bonds at all; in EL2 and EL3 phenol was a donor of the hydrogen bond (Fig. 5).

It appeared that in molecular dynamics trajectories, which evolved from EL1 and EL2, position of phenol in

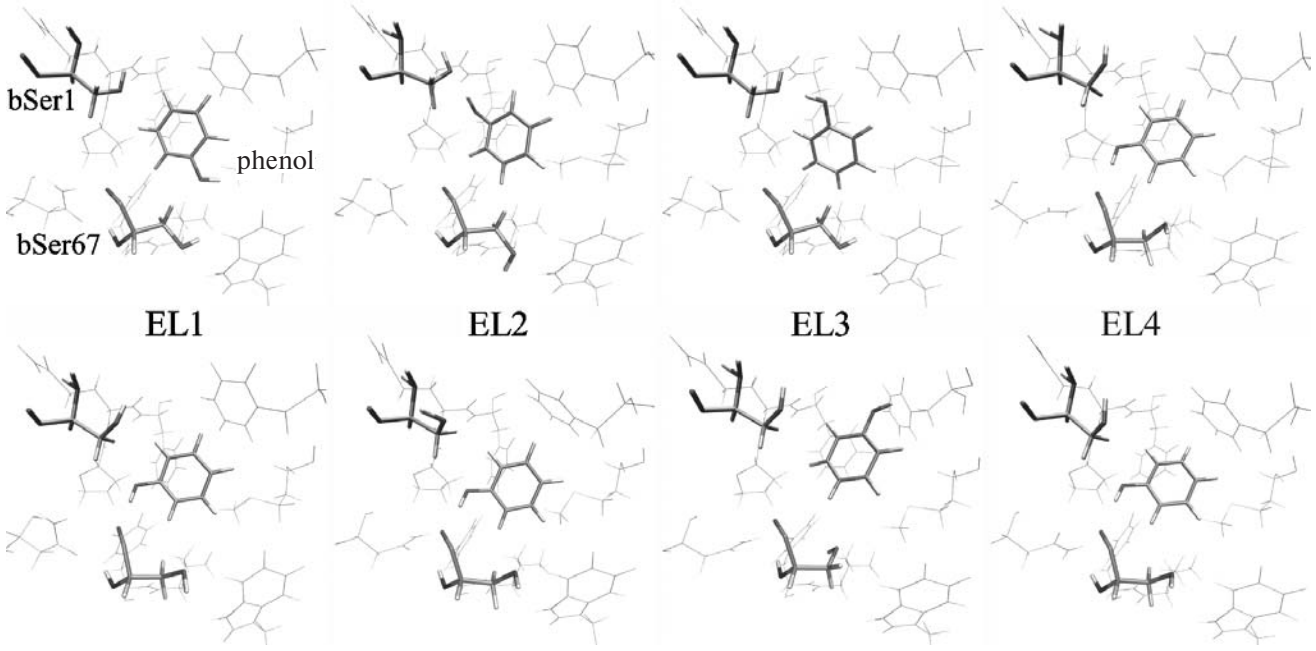

Fig. 5. Starting (top row) and MD (bottom row) structures of enzyme–phenol complex.

the active site switched to the same mode as in EL4, with the hydrogen bond between the phenol hydroxyl and the main chain oxygen of bS67. EL4 appeared to represent steady binding mode: RMSD of the phenol molecule was 0.51 Å, with RMSF of 0.7 Å, and occupancy of the hydrogen bond was 98%. Although in a found binding mode phenol molecule was indeed placed with its hydroxyl group at the bottom of the hydrophobic pocket, its orientation qualitatively differed from 1AI7, clearly pointing to the hydrogen bond with main chain oxygen of bS67. Specific interaction with the main chain oxygen of b67 residue could be also conserved in PA from *A. faecalis*: despite serine being replaced by alanine, all other residues comprising the hydrophobic pocket are conserved, and the active site structure, as homology modeling shows, has much similarity with that of *E. coli*.

The EL3 trajectory has shown somewhat different behavior. Initially phenol molecule was oriented with its hydroxyl group towards solution and formed hydrogen bond with bS1 (Fig. 5). After EL3 system was pre-equilibrated and constraints were taken off, the phenol molecule switched to a position identical with that observed in EL1, EL2, and EL4 trajectories. However, after 350 psec the ligand changed its position again, i.e. it flipped back to expose its hydroxyl group to solution and lost its hydrogen bonds with the enzyme. This event was accompanied by the conformational transition of residues aR145 and aF146, which switched to the "open" conformation. Since phenol is a specific inhibitor of the PA, and X-ray picture of its complex with the enzyme clearly indicates the presence of a "closed" active site conformation, we might suggest that EL3 trajectory could rather represent pre-dissociation state of phenol than its steady binding mode. Following these considerations unbinding of phenol proceeds via a consequence of events, comprising cooperative opening of the hydrophobic bottleneck, removal of specific contacts (hydrogen bonds) with the protein and retaining only nonspecific hydrophobic contacts.

Conformational transitions in the active site governing substrate binding. Molecular dynamics studies of the enzyme–phenol complex raised new aspects of the role of conformational mobility of the active site residues (aR145 and aF146) involved in ligand binding. Historically, crystal structures of PA complexes with its inhibitors have been divided into two subsets, with and without conformational transition of the side chains of aR145 and aF146 residues [12]. It was stated that by exposing these residues to solution it became possible to accommodate nonspecific, bulky ligands in the active site of the enzyme; also a suggestion was made that "opening" could serve as a general gateway mechanism governing substrate binding. However, conclusions derived from crystallographic data were significantly restricted by their static nature. According to available crystal structures of PA [10, 12-14], residues aR145 and aF146 are located at the end of a 16-residue helix beginning with aP131. However, secondary structure assignment of this region reveals that entirely α-helical region ends at aM142. The next residue, aA143, represents a borderline case between α- and π-helical regions; residue aN144 is in pure α-helical conformation, while the main chain of aR145, being severely

distorted, cannot be attributed to a certain secondary structure motif. In "closed" structures aF146 is in α-helical, while in "open" ones it switches to π-helical conformation. This observation leads to the conclusion that switching between "closed" and "open" conformations is not restricted only to side chain movements of aR145 and aF146, but is accompanied by C_α-atom movements of residues a144-a146 and change of hydrogen bonding pattern of aF146 (Fig. 6a, see color insert).

Analysis of conformational dynamics of a143-a146 coil region reveals that movements of aR145 and aF146 side chains are rather a "facade" of the phenomenon than its "foundation". Separate observations of "closed" (free enzyme; complexes ES2 and ES3 with PG; complexes EL1, EL2, EL4 with phenol; complex with phenylacetic acid) and "open" (complex ES1 with PG) states, as well as transition between these conformations observed in the molecular dynamics trajectory of EL3 complex with phenol, extended the notion of "opening". First, it appeared that "closed" conformation was tolerant with respect to C_α displacements of residues aN144 and aR145. Several trajectories (free enzyme; EL1, EL2, and EL4 complexes with phenol; complex with phenylacetic acid) revealed that positions of C_α atoms of residues a143-a146 were well conserved with respect to crystallographic structures (Fig. 6b). At the same time, trajectories ES2 and ES3 presenting enzyme complex with bulkier ligand, PG, were characterized by the shift of aN144 and aR145 C_α atoms, but positions of the side chains of a143-a146 coil remained intact.

What especially distinguished trajectories of "open" structures was the aF146 C_α atom shift from the "closed" backbone pattern, which took place in addition to displacements of aN144 and aR145 residues. A crucial qualitative trait of this displacement was that it caused reorganization of the hydrogen bonding pattern of the aF146 main chain: while residues aN144 and aR145 preserved hydrogen bonds inherent for the "closed" state, residue aF146 formed a new bond with the main chain oxygen of aT141 instead of aM142, and thus has moved from α- to π-helical state. It may be tentatively suggested that formation of this hydrogen bond may stabilize C_α shift of aF146 and anchor the "open" conformation, since "opening" of the residue aF146 and its exposition towards solution is restricted to the rigid movement of the residue as a whole, preserving its side chain conformation. At the same time, "opening" of aR145 implies both C_α shift and conformational transition of its side chain from trans to gauche-(+).

Observation of the EL3 molecular dynamics trajectory uncovered the consequence of events accompanying transition of the a143-a146 coil region from the "closed" to "open" state and transition of the phenol molecule to pre-dissociation conformation. The first event in this series is the shift of aR145 C_α atom and anchoring this new position by the hydrogen bond between the main chain amide of aR145 and oxygen of aA143. Then the side chain of aR145 bends and guanidine group of the arginine moves towards solution. However, this conformation can be still distinguished form the "open" state, since aF146 holds its initial position. This "partially open" state, with aR145 exposed to solution, remains stable during approximately 500 psec of the molecular dynamics trajectory, and thus can be regarded as an intermediate on the pathway from "closed" to "open" conformation. Finally, C_α atom of aF146 shifts and its hydrogen-bonding pattern switches to a state characteristic for π-helical conformation. Transition to the "open" state is completed.

Analysis of observed conformational transition suggests that region a143-a146 seems to be unstructured not by chance—it needs conformational flexibility at least in a few degrees of freedom to trigger the substrate binding. Bottleneck of the hydrophobic pocket in the native enzyme is too narrow to accommodate the acyl moiety of the substrate, and reversible conformational gating of the residues comprising the wall and partially the bottleneck of the hydrophobic cavity allows transmission of the substrate and its tight binding. Some of the substrates, especially those with bulky substituents in the acyl moiety and those of an "improper" shape, may prohibit reversible "closure" of the bottleneck, freezing the "open" conformation. However, mechanical gating of the substrate binding may not exhaust the conformational role of these residues in PA catalysis. Recent studies [29, 30] concerning the catalytic activity of aR145 and aF146 mutants witness that conformational properties of this "unstructured" region are also crucial for maintaining the catalytic framework.

Thus, molecular modeling has brought up intimate details of the mechanism of binding of natural substrate, penicillin G, in the PA active site and solved questions raised by analysis of available X-ray structures mimicking Michaelis complex. Molecular modeling pointed out additional contacts of penicillin G with residues bG385, bS386, and bN388, which were missing in X-ray structures. Combination of molecular docking and molecular dynamics also clarified the nature of extremely effective phenol binding in the hydrophobic pocket of PA, which lacked proper explanation from crystallographic experiments. The current investigation has sufficiently extended our knowledge of the nature of the conformational transition in the a143-a146 coil region coupled to substrate binding and release of the reaction products.

This work was supported by the Russian Foundation for Basic Research (grant 06-04-49312).

REFERENCES

1. Rolinson, G. N., Batchelor, F. R., Butterworth, D., Cameron-Wood, J., Cole, M., Eustace, G. C., Hart, M. V., Richards, M., and Chain, E. B. (1960) *Nature*, **187**, 236-237.

2. Margolin, A. L., Švedas, V. K., and Berezin, I. V. (1980) *Biochim. Biophys. Acta*, **616**, 283-289.
3. Roa, A., Castillon, M. P., Goble, M. L., Virden, R., and Garcia, J. L. (1995) *Biochem. Biophys. Res. Commun.*, **206**, 629-636.
4. Bruggink, A., Roos, E. C., and de Vroom, E. (1998) *Org. Process Res. Dev.*, **2**, 128-133.
5. Švedas, V. K., Savchenko, M. V., Beltser, A. I., and Guranda, D. F. (1996) *Ann. N.-Y. Acad. Sci.*, **799**, 659-669.
6. Guranda, D. T., van Langen, L. M., van Rantwijk, F., Sheldon, R. A., and Švedas, V. K. (2001) *Tetrahedron: Asymmetry*, **12**, 1645-1650.
7. Chilov, G. G., and Švedas, V. K. (2002) *Can. J. Chem.*, **80**, 699-707.
8. Ferreira, J. S., Straathof, A. J. J., Franco, T. T., and van der Wielen, L. A. M. (2004) *J. Mol. Catalysis B: Enzymatic*, **27**, 29-35.
9. Chilov, G. G., Moody, H. M., Boesten, W. H. J., and Švedas, V. K. (2003) *Tetrahedron: Asymmetry*, **14**, 2613-2617.
10. Duggleby, H. J., Tolley, S. P., Hill, C. P., Dodson, E. J., Dodson, G., and Moody, P. C. (1995) *Nature*, **373**, 264-268.
11. Brannigan, J. A., Dodson, G., Duggleby, H. J., Moody, P. C., Smith, J. L., Tomchick, D. R., and Murzin, A. G. (1995) *Nature*, **378**, 416-419.
12. Done, S. H., Brannigan, J. A., Moody, P. C. E., and Hubbard, R. E. (1998) *J. Mol. Biol.*, **284**, 463-475.
13. Alkema, W. B. L., Hensgens, C. M. H., Kroezinga, E. H., de Vries, E., Floris, R., van der Laan, J.-M., Dijkstra, B. W., and Janssen, D. B. (2000) *Protein Eng.*, **13**, 857-863.
14. McVey, C. E., Walsh, M. A., Dodson, G. G., Wilson, K. S., and Brannigan, J. (2001) *J. Mol. Biol.*, **313**, 139-150.
15. Berendsen, H. J. C., van der Spoel, D., and van Drunen, R. (1995) *Comp. Phys. Comm.*, **91**, 43-56.
16. Lindahl, E., Hess, B., and van der Spoel, D. (2001) *J. Mol. Mod.*, **7**, 306-317.
17. Jorgensen, W. L., and Tirado-Rives, J. (1988) *J. Am. Chem. Soc.*, **110**, 1657-1666.
18. Jorgensen, W. L., Chandrasekhar, J. D., Madura, R., Impey, W., and Klein, M. L. (1983) *J. Chem. Phys.*, **79**, 926-935.
19. Feenstra, K. A., Hess, B., and Berendsen, H. J. C. (1999) *J. Comp. Chem.*, **20**, 786-798.
20. Hess, B., Bekker, H., Berendsen, H. J. C., and Fraaije, J. G. E. M. (1997) *J. Comp. Chem.*, **18**, 1463-1472.
21. Tironi, I. G., Sperb, R., Smith, P. E., and van Gunsteren, W. F. (1995) *J. Chem. Phys.*, **102**, 5451-5459.
22. Shmidt, M. W., Baldringe, K. K., Boatz, J. A., Elbert, S. T., Gordon, M. S., Jensen, J. H., Koseki, S., Matsunaga, N., Nguyen, K. A., Su, S. J., and Windus, T. L. (1993) *J. Comp. Chem.*, **14**, 1347-1363.
23. Granovsky, A. A., http://www.classic.chem.msu.su/gran/gamess/index.html
24. Bayly, C. L., Cieplak, P., Cornell, W. D., and Kollman, P. A. (1993) *J. Phys. Chem.*, **97**, 10269-10280.
25. Stroganov, O. V., Chilov, G. G., and Švedas, V. K. (2003) *J. Mol. Structure (THEOCHEM)*, **631**, 117-125.
26. Morris, G. M., Goodsell, D. S., Halliday, R. S., Huey, R., Hart, W., Belew, R. K., and Olson, A. J. (1998) *J. Comp. Chem.*, **19**, 1639-1662.
27. Chilov, G. G., Sidorova, A. V., and Švedas, V. K. (2007) *Biochemistry (Moscow)*, **72**, 495-500.
28. Chilov, G. G., Guranda, D. T., and Švedas, V. K. (2000) *Biochemistry (Moscow)*, **65**, 963-966.
29. Alkema, W. B. L., Prins, A. K., de Vries, E., and Janssen, D. B. (2002) *Biochem. J.*, **365**, 303-309.
30. Alkema, W. B. L., Dijkhuis, A.-J., de Vries, E., and Janssen, D. B. (2002) *Eur. J. Biochem.*, **269**, 2093-2100.